Dynamic change of Ice Flow Velocity in Holmes Glacier Since the 1970s

Shi Li^{1,2}; Guojun Li^{1,2}, Yuan Cheng^{3*}, Xuehui Pi^{1,2*}, Rongxing Li^{1,2}

¹Center for Spatial Information Science and Sustainable Development Applications, Tongji University, 1239 Siping Road, Shanghai 200092, China – (2333621@tongji.edu.cn, liguojunlee@tongji.edu.cn, pixh@tongji.edu.cn, rli@tongji.edu.cn)

²College of Surveying and Geo-Informatics, Tongji University, 1239 Siping Road, Shanghai, China

³Institute for the Conservation of Cultural Heritage, School of Cultural Heritage and Information Management, Shanghai University, 99 Shangda Road, Shanghai, 200444, China-chengyuan@shu.edu.cn

Keywords: Historical Ice Velocity, Dynamic Change, Holmes Glacier.

Abstract

The Holmes Glacier is a major outlet glacier in Wilkes Land, East Antarctica, a region experiencing accelerated ice mass loss. To study the historical dynamic changes of the Holmes Glacier in East Antarctica, this study utilized Landsat MSS imagery to reconstruct a high-resolution velocity map of the glacier dating back to the 1970s. Our results reveals that the Holmes Glacier has experienced a long-term acceleration trend on its ice shelf since the 1970s, a trend that corresponds with observed ice shelf thinning and basal melting. Concurrently, there was no significant acceleration near the grounding line of Holmes West, whereas Holmes East showed marked acceleration, reflecting different conditions of modified Circumpolar Deep Water (mCDW) intrusion at the grounding lines of the two ice streams. A calving event was identified in March 2021, which occurred significantly earlier than previous events in its historically stable cycle, possibly indicating the reduced stability of the Holmes Ice Shelf. The high-resolution historical velocity data provided by this study reveal that the Holmes Glacier has shown an overall trend of destabilization and mass loss during the observation period. The study concludes that the observed acceleration is primarily driven by the basal melting of the ice shelf, which is caused by the intrusion of warm ocean water and the subsequent thinning of the ice shelf, provide a new historical perspective on the dynamics of Holmes glacier.

1. Introduction

The mass loss from the Antarctic Ice Sheet is one of the most significant contributors to global sea-level rise (Smith et al., 2020), with the ice shelves are experiencing widespread acceleration and volume loss (Paolo et al., 2015). In addition to the West Antarctic Ice Sheet, the East Antarctic Ice Sheet (EAIS) has also become a major contributor in recent years. Its accelerated mass loss is attributed to increased ice discharge from several ocean-driven ice shelves in the Wilkes Land region (Rignot et al., 2019). The Holmes Glacier system, a major outlet glacier in Porpoise Bay, Wilkes Land, is a key component for understanding the dynamic response of the EAIS to ongoing climate change.

Wilkes Land has been identified as a region undergoing accelerated ice mass loss, contributing significantly to the overall mass balance of the EAIS. It exhibits a high sensitivity to marine ice sheet instability due to its grounding line being predominantly below sea level and the presence of deep subglacial troughs that facilitate oceanic forcing (Weertman, 1974; Schoof, 2007; Young et al., 2011; Klose et al., 2024). Furthermore, this broader context identifies Wilkes Land as a "warm-shelf" region susceptible to the intrusion of modified Circumpolar Deep Water (mCDW) (Picton et al., 2023). This raises concerns about the potential role of ocean-driven basal melting in influencing the stability and long-term behavior of the Holmes Glacier.

It has been observed that calving events or a reduction in the thickness of ice shelves can dramatically accelerate ice flow (Scambos et al., 2004; Rydt et al., 2015). The history of large-scale and intermittent calving events observed since the 1960s is

crucial for understanding the dynamics of the Holmes Glacier. Events such as those in 2007 and 2016 are closely linked to the stability and breakup of landfast sea ice in Porpoise Bay, which typically acts as a buttressing agent. The mechanisms driving sea ice breakup appear to be diverse; some events are linked to atmospheric preconditioning, while others are related to the glacier's own advance disrupting the sea ice front (Miles et al., 2017).

Research using satellite altimetry has clearly identified the Holmes Glacier as one of the floating ice systems in East Antarctica that experienced net thinning between 2003 and 2008. This thinning was attributed to enhanced basal melt, driven primarily by ocean interactions (Pritchard et al., 2012). And the observed reduction of three pinning-points on the Holmes Ice Shelf between 1973 and 2022 further underscores the long-term thinning process of the ice shelf. (Miles et al., 2024). Wilkes Land's regional oceanographic context strongly suggest that ocean forcing is a plausible and important factor in its long-term dynamics (Picton et al., 2023).

A comprehensive understanding of the full evolutionary history of the Holmes Glacier is challenged by a scarcity of historical data. While modern satellite data facilitate the systematic analysis of recent changes, such as landfast sea ice disintegration, front position, and thickness. However, due to the lack of image materials, systematic and high-resolution records of glacier velocity prior to the 1980s are missing (Li et al., 2022). Similarly, direct measurements of oceanographic conditions and grounding line changes specific to the glacier are limited. Although indirect evidence suggests that the Holmes Ice Shelf experienced an acceleration, a continuous, basin-wide quantitative velocity field

^{*} Corresponding author

that could confirm this phenomenon remains absent. Current research is primarily focused on the developments of the past two to three decades, while analyses involving the earlier historical period are generally constrained by the low resolution and discontinuous spatiotemporal coverage of observational data. This lack of a long-term observational record constitutes a major obstacle to our comprehensive understanding of the change and response mechanisms of the Holmes Glacier (Li et al., 2023).

Therefore, this study aims to: (1) systematically reconstruct ice velocity maps for the region from the 1970s from Landsat MSS via image matching and photogrammetry techniques, and quantify decadal-scale changes by comparing with modern velocities; (2) extract and analyse ice front positions to identify calving events, critical for assessing instability of the ice shelf; and (3) investigate the linkages between the glacier's dynamic evolution and ocean thermal forcing. By investigating these historical dynamic characteristics, a more systematic understanding of the response patterns and mechanisms of glaciers in this region to environmental forcing can be obtained.

2. Study Area and Date

2.1 Study Area

The study area is centred on the Holmes Glacier system, located in Wilkes Land, East Antarctica. It debouches into the western part of Porpoise Bay at approximately 66°46′S, 126°54′E (Figure 1). Porpoise Bay is a 150 km wide embayment typically filled with multi-year landfast sea ice (Fraser et al., 2012). The glacier system includes two main ice flows, Holmes West and Holmes East, with the primary focus often on the Holmes West Glacier, the widest outlet glacier feeding into the bay. This region is of significant glaciological interest as Wilkes Land overlies the Aurora Subglacial Basin. It has been identified as an area experiencing accelerated mass loss and dynamic changes, sometimes referred to as the "weak underbelly" of the East Antarctic Ice Sheet due to its marine-based grounding lines and deep subglacial troughs, which can facilitate oceanic forcing (Picton et al., 2023; Miles et al., 2017).

2.2 Date

This study draws upon a suite of historical and contemporary imagery. The 1970s velocity map were reconstructed using Landsat MSS imagery (1972–1973, 60 m optical resolution). The calving event after 2016 was identified using Landsat OLI imagery. The RADARSAT imagery was used to identify front position in 1997. The Landsat data were downloaded from the USGS Landsat distribution site (https://earthexplorer.usgs.gov/), and RADARSAT data from the Alaska Satellite Facility

distribution site (https://search.asf.alaska.edu/). These imageries used in this study are listed in Table 1. Topographic and geometric corrections on Landsat MSS imagery relied on the Landsat Image Mosaic of Antarctica (LIMA) (Bindschadler et al., 2018) and the RADARSAT-1 Antarctic Mapping Project (RAMP) v2 Digital Elevation Model (DEM) (H. Liu et al., 2015). For modern velocity references, NASA MEaSURES ITS_LIVE products were utilized, including Version 2 (120 m resolution) and Version 1 (240 m resolution) (Mouginot et al., 2017; Gardner et al., 2018, Gardner et al., 2022; Lei et al., 2021; Lei et al., 2022).

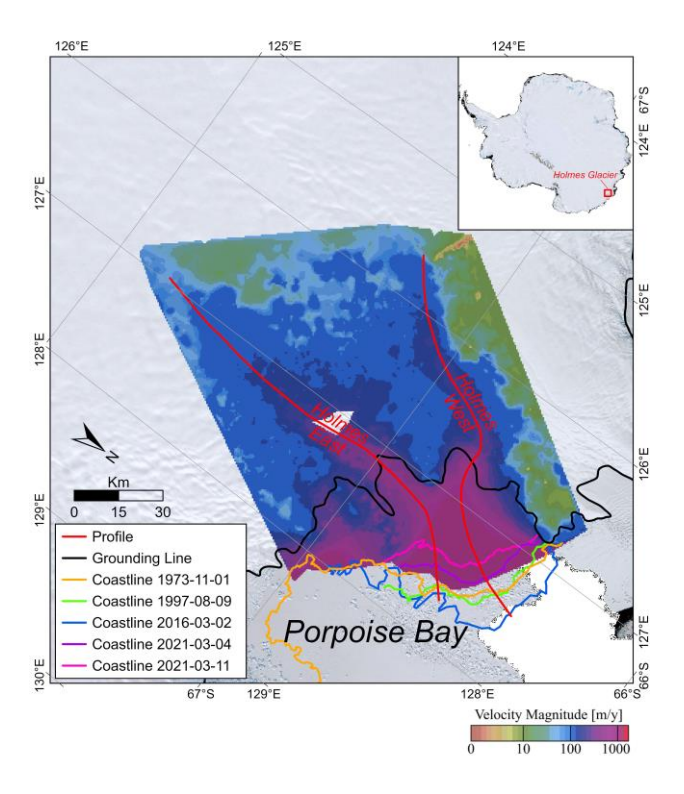


Figure 1 Study area map of Holmes Glacier, East Antarctica. Holmes Glacier is highlighted in the inset map. Main map Background shows historical ice velocity map (1972-1973) reconstructed in this study. Features include velocity profile lines, grounding line (Gardner et al., 2018), coastlines. It should be noted that the coastline positions 1973 and 1997 do not represent the coastline positions at the exact time of calving events. The background was provided by the LIMA.

Satellite	Imagery	Date of imagery	Usage in in this study
Landsat MSS	LM11001071972350AAA05	1972-12-15	Reconstruct historical ice velocity map
Landsat MSS	LM10981081973001XXX01	1973-01-01	Reconstruct historical ice velocity map
Landsat MSS	LM10961071973305AAA05	1973-11-01	Reconstruct historical ice velocity map
RADARSAT-1	R1_09207_SWB_F623	1997-08-09	Identify front position
Landsat OLI	LC80941072021063LGN00	2021-03-04	Identify front position
Landsat OLI	LC80951072021070LGN00	2021-03-11	Identify front position

Table 1 Satellite Imagery used in the study

The selection of the profile lines was guided by several datasets. The Reference Elevation Model of Antarctica (REMA) (Howat et al., 2019) achieving 2-meter resolution with meter-level accuracy across most regions. In addition to the multi-year ice velocity maps mentioned above, we also incorporated the MEaSUREs InSAR-based Antarctica velocity map (Rignot, 2017), which provides the velocity over the long-term span from 1996 to 2016. Ice flowlines (Y. Liu et al., 2015) and the positions of the ice front were also considered.

Then analysis incorporated the ITS_LIVE Antarctic ice shelf basal melt rate dataset (NSIDC-0792; 1920 m resolution; quarterly, 1992–2017) (Paolo et al., 2024). This dataset provides the basal melt rate and thickness data in Holmes ice shelf. These information on ice velocity, ice shelf front position, thickness change, and basal melt, covering both historical and contemporary eras.

3. Methodology

3.1 Reconstructing Historical Ice Velocities

The historical ice velocity map was reconstructed using early digital imagery from Landsat 1. As early Landsat historical satellite imagery lacks correct georeferencing information, preprocessing steps such as georegistration and orthorectification were required prior to ice velocity extraction. The imageries were registered to the LIMA mosaic and the RAMP v2 DEM using stable Ground Control Points (GCPs) which on stationary landmarks, including rock outcrops and blue ice features and others. A bundle block adjustment was then used to refine the exterior orientation parameters of the images, resulting in orthorectified imagery referenced to WGS 84 and the Antarctic Polar Stereographic projection (EPSG:3031). For our target region in East Antarctica, we achieved an orthorectification accuracy of better than one native pixel.

Ice velocity extraction primarily employed feature tracking, with the historical glacier velocity map constructed via a hierarchical and dynamically densifying network (Li et al., 2017; Feng et al., 2023). First, at the top level of a low-resolution image pyramid, an initial velocity map structure was built by manually selecting and matching seed points in both slow- and fast-flowing regions. Normalized Cross-Correlation (NCC) was then used to match ice surface features, and a Triangulated Irregular Network (TIN) model was used to constrain the matching process. Within the TIN model, matched points from the preceding layer were used to predict and constrain the search range for new feature points, with recursive feature matching and tracking performed layer by layer. This process progressively establishes a dynamically dense network of displacement vectors and generates a gridded velocity map point.

To improve the matching success rate and sub-pixel positioning accuracy, we adopted a multi-scale matching strategy and an Adaptive Histogram Equalization image enhancement technique. Outlier vectors were removed using a dual-threshold technique on the correlation coefficient and by enforcing consistency of velocity and direction within the local neighbourhood, ensuring the final velocity map possessed both high density and high reliability (Feng et al., 2023).

Finally, the ice flow velocity error was estimated by combining the orthorectification errors, feature identification error, matching error, and the image time interval (Feng et al., 2023), as shown in equation (1):

$$\sigma_{vlc} = \frac{1}{\Delta t} \sqrt{\sigma_{ref}^2 + \sigma_{src}^2 + \sigma_{idn}^2 + \sigma_{mtc}^2}$$
 (1)

where σ_{vlc} = ice flow velocity error

 $\Delta t = \text{time span between two images}$

 σ_{ref} , σ_{src} = the geolocation uncertainties of the reference and search orthoimages

 $\sigma_{idn}\!=feature\ identification\ accuracy$

 σ_{mtc} = feature matching accuracy

For the final generated grid velocity points, we calculated their theoretical error by defining the components as follows: σ_{ref} and σ_{idn} were set to 0, σ_{src} was set to 1 pixel, and σ_{mtc} was set to 0.25 pixels, based on the maximum pixel resolution of the imagery used

3.2 Integrating ITS_LIVE Date

For the contemporary period, we used the ITS_LIVE velocity dataset (Lei et al., 2021; Gardner et al., 2022), which provided the complete annual velocity data of the Holmes Glacier since 2013 and the corresponding image-pair velocity data. Due to significant errors in the 2021 annual velocity data near the ice front, we refit the annual maps using Gardner's original synthesis method (an error-weighted average) (Gardner et al., 2018). Prior to this refitting, we manually filtered Gardner's pair data to remove pairs with high errors (approximately 300 m/yr) or velocity maps that were identified as clear outliers.

3.3 Profile line Selection

To quantitatively analyse the spatial and temporal changes in ice velocity and identify the main mass transport pathways, we selected representative profile lines. The incorrect placement of profile lines may result in extracted velocities that fail to represent the dynamic characteristics of the ice shelf. First, the location of the main ice flow was determined based on the width and length of the high-velocity region in the multi-year velocity fields. An initial profile line was then established by ice flowline data

The initial profile was followed by a fine-tuning process, where we used the REMA DEM in a 3D environment, overlaying it with the velocity maps for visual inspection of the initial profile line. Within the glacierized region, the profile line must follow the valley in the DEM and run parallel to the ice flowlines. The ice front positions were primarily used to ensure that the downstream portion of the profile line was centrally located on the ice front. The starting point of the profile line was defined by the $\sim\!80$ m/yr velocity line, while its end point was set at the most advanced ice front from the different time periods, to encompass velocity data from all periods.

Since published ice velocity products are raster data, we generated sampling points at 1 km intervals along this profile. For each sampling point, we created a 750 m radius buffer zone and calculated the mean ice velocity within it. Finally, we applied a 15 km moving average smoothing to these extracted values to analyse the average velocity changes on the ice shelf.

3.4 Analysing Ice Shelf Dynamics

For the ice front analysis, we referenced the work of Miles (Miles et al., 2017), which provided an analysis of the front position from 1963 to 2016. In this study, we used Landsat imagery to identify major calving events after 2016. We then investigated the long-term glacio-dynamic context of the Holmes Ice Shelf by integrating publicly available datasets. The MEaSUREs

ITS_LIVE Antarctic Quarterly 1920 m Ice Shelf Height Change and Basal Melt Rates dataset (NSIDC-0792) provided insights into basal melt rates and ice shelf thickness. To mitigate short-term fluctuations, the ice shelf thickness dataset was initially averaged into three-month intervals. Subsequently, the long-term trend was estimated using a low-order polynomial fit (n \leq 3) combined with Lasso regularization regression and a cross-validation method.

4. Results

The Holmes Glacier exhibits a clear trend of acceleration on ice shelf area. Reconstructed historical velocity data from the 1970s along the profile line are lower than modern measurements from ITS_LIVE. The reconstructed ice shelf profile velocity data reveals that the average acceleration along the two Holmes Ice Shelf profiles from 1973 to 2014 was 70 ± 60 m/yr. Although the large theoretical velocity error stems from the 11-month interval between 1973 imagery acquisitions, it can be considered that 21st-century ice flow has significantly accelerated compared to its historical state within this error range. This acceleration is closely linked to changes in the glacier's mass balance. Ice shelf thickness data (Figure 2) reveal that the Holmes Ice Shelf underwent overall thinning from 1992 to 2018, which corresponds with the acceleration observed across the ice shelf.

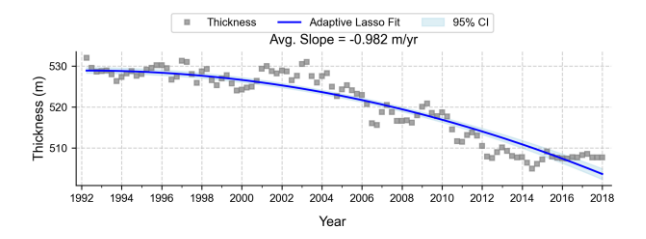


Figure 2 Ice shelf thickness time series (1992-2017) from ITS LIVE NSIDC-0792 dataset. Holmes ice shelf shows a thinning trend (approximately 0.982 m/yr).

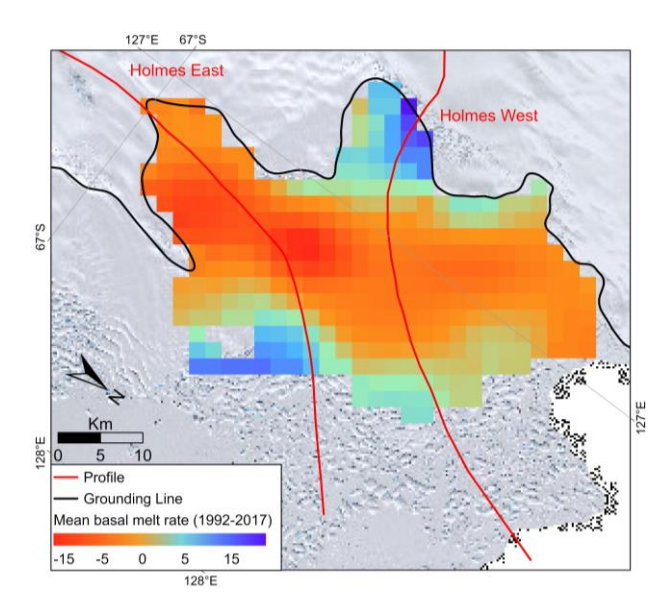


Figure 3 Mean basal melt rate (1992-2017) from ITS LIVE NSIDC-0792 dataset. The ice shelf base near the grounding line of Holmes East is in a state of melting, while the base of Holmes West is frozen.

As shown in Figure 3, basal melting at the grounding line of Holmes West is positive, whereas at Holmes East it is negative. This corresponds with the velocity map, which shows no acceleration at the Holmes West grounding line but indicates acceleration near the grounding line of Holmes East. Away from the grounding line, distinct melt zones are evident on the ice shelf, leading to the thinning. Data from Adusumilli et al. (2020) shows that basal melt rates in this region reached 13 ± 2.9 m/yr between 1994 and 2018. These suggest the intrusion of warm ocean water and dynamic changes triggered by thinning, which have contributed to the observed velocity increase. A mass balance assessment for the period 1979–2018 shows a cumulative balance of -152 Gt in Holmes Glacier (Rignot et al., 2019), which is broadly consistent with the observed acceleration and thinning.

Refitting the ITS_LIVE 2021 annual maps reduced the mean error on ice shelf along the profile line from 115 m/yr to 32 m/yr. The average acceleration from 2014 to 2021 was 52 ± 24 m/yr. The acceleration seen in 2021 is associated with a calving event in the same year. The Holmes Ice Shelf experienced major calving events during 1982–1986, 1999–2001, and 2016 (Miles et al., 2017), with another event observed in March 2021 in this study (Figure 1). While the exact timing of the first two events could not be determined due to a lack of imagery. The ice shelf appears to follow an approximately 15-year calving cycle, with the calving front breaking off at roughly the same location (Miles et al., 2017). However, the 2021 calving event occurred prematurely, before the ice front had readvanced to its previous position. This premature calving is likely linked to increased ice shelf instability resulting from thinning.

5. Conclusion

In this study, we reconstruct the 1972–1973 ice flow velocity of the Holmes Ice Shelf and identify its 2021 calving event. We then compare this historical velocity with current observations, incorporating data on the calving events, ice shelf thickness, and basal melt rates to evaluate the long-term dynamics.

The results reflect that the ice shelf has exhibited significant acceleration over the past few decades, which is linked to increased instability caused by ice shelf thinning that was driven by basal melting. And the two main ice streams of Holmes Glacier are subject to differential warm water intrusion near their grounding lines, with Holmes East being more affected. The premature of the 2021 calving event suggests an increase in the instability of the Holmes Glacier. These findings provide a new understanding of the evolutionary development of Holmes Glacier, revealing that the glacier has been in a state of continuous mass loss and trending towards instability throughout the observational period.

Acknowledgements

This work has been supported by the Natural Science Foundation of China (No.42394131, 42301149) and the National Key Research & Development Program of China (No.2021YFB3900105, 2017YFA0603100). We would like to thank the United States Geological Survey (USGS) for providing the Landsat images used in this study. We thank the ITS LIVE project for providing the comprehensive ice velocity datasets, thickness data, basal melt rate data and code for fit annual velocity data that enabled this research. We also extend our sincere gratitude to the institutions and research teams for providing their invaluable data. This research would not have been possible without their support.

References

- Adusumilli, S., Fricker, H. A., Medley, B., Padman, L., & Siegfried, M. R, 2020. Interannual variations in meltwater input to the Southern Ocean from Antarctic ice shelves, *Nature geoscience*, 13, 616–620.
- Bindschadler, R., Vornberger, P., Fleming, A., Fox, A., Mullins, J., Binnie, D., Paulson, S., Granneman, B., and Gorodetzky, D., 2008. The Landsat Image Mosaic of Antarctica. *Remote Sensing of Environment*, 112(12), pp. 4214-4226.
- De Rydt, J., Gudmundsson, G. H., Rott, H., & Bamber, J. L, 2015 Modeling the instantaneous response of glaciers after the collapse of the Larsen B Ice Shelf. *Geophysical Research Letters*, 42(13), 5355-5363.
- Feng, T., Li, Y., Wang, K., Qiao, G., Cheng, Y., Yuan, X., ... & Li, R, 2023. A hierarchical network densification approach for reconstruction of historical ice velocity fields in East Antarctica. *Journal of Glaciology*, 69(274), 281-300.
- Fraser, A. D., Massom, R. A., Michael, K. J., Galton-Fenzi, B. K., & Lieser, J. L, 2012. East Antarctic landfast sea ice distribution and variability, 2000–08. *Journal of Climate*, 25(4), 1137-1156.
- Gardner, A. S., Fahnestock, M. & Scambos, T, 2022. MEaSURES ITS_LIVE Regional Glacier and Ice Sheet Surface Velocities. (NSIDC-0776, Version 1). [Data Set]. Boulder, Colorado USA. NASA National Snow and Ice Data Center Distributed Active Archive Center. doi.org/10.5067/6II6VW8LLWJ7. Date Accessed 04-25-2025.
- Gardner, A. S., Moholdt, G., Scambos, T., Fahnstock, M., Ligtenberg, S., Van Den Broeke, M., & Nilsson, J. 2018. Increased West Antarctic and unchanged East Antarctic ice discharge over the last 7 years. *The Cryosphere*, *12*(2), 521-547.
- Howat, I. M., Porter, C., Smith, B. E., Noh, M. J., & Morin, P, 2019. The reference elevation model of Antarctica. *The Cryosphere*, *13*(2), 665-674.
- Klose, A. K., Coulon, V., Pattyn, F., & Winkelmann, R., 2024. The long-term sea-level commitment from Antarctica. *The Cryosphere*, 18(9), 4463-4492.
- Lei, Y., Gardner, A., & Agram, P, 2021. Autonomous repeat image feature tracking (autoRIFT) and its application for tracking ice displacement. *Remote Sensing*, 13(4), 749.
- Lei, Y., Gardner, A. S., & Agram, P, 2022. Processing methodology for the ITS_LIVE Sentinel-1 ice velocity products. *Earth System Science Data*, 14(11), 5111-5137.
- Li, R., Cheng, Y., Chang, T., Gwyther, D. E., Forbes, M., An, L., ... & Ye, W, 2023. Satellite record reveals 1960s acceleration of Totten Ice Shelf in East Antarctica, *Nature Communications*, 14, 4061.
- Li, R., Cheng, Y., Cui, H., Xia, M., Yuan, X., Li, Z., ... & Qiao, G, 2022. Overestimation and adjustment of Antarctic ice flow velocity fields reconstructed from historical satellite imagery. *The Cryosphere*, *16*(2), 737-760.
- Li, R., Ye, W., Qiao, G., Tong, X., Liu, S., Kong, F., & Ma, X, 2017. A new analytical method for estimating Antarctic ice flow

- in the 1960s from historical optical satellite imagery. *IEEE Transactions on Geoscience and Remote Sensing*, 55(5), 2771-2785
- Liu, H., Jezek, K. C., Li, B. & Zhao, Z, 2015. Radarsat Antarctic Mapping Project Digital Elevation Model. (NSIDC-0082, Version 2). [Data Set]. Boulder, Colorado USA. NASA National Snow and Ice Data Center Distributed Active Archive Center. doi.org/10.5067/8JKNEW6BFRVD. Date Accessed 04-25-2025.
- Liu, Y., Moore, J. C., Cheng, X., Gladstone, R. M., Bassis, J. N., Liu, H., ... & Hui, F, 2015. Ocean-driven thinning enhances iceberg calving and retreat of Antarctic ice shelves. *Proceedings of the National Academy of Sciences*, 112(11), 3263-3268.
- Miles, B. W., & Bingham, R. G, 2024. Progressive unanchoring of Antarctic ice shelves since 1973. *Nature*, 626(8000), 785-791.
- Miles, B. W., Stokes, C. R., & Jamieson, S. S, 2017. Simultaneous disintegration of outlet glaciers in Porpoise Bay (Wilkes Land), East Antarctica, driven by sea ice break-up. *The Cryosphere*,11(1), 427-442.
- Mouginot, J., Rignot, E., Scheuchl, B., & Millan, R, 2017. Comprehensive annual ice sheet velocity mapping using Landsat-8, Sentinel-1, and RADARSAT-2 data. *Remote Sensing*, 9(4), 364.
- Paolo, F. S., Fricker, H. A., & Padman, L, 2015. Volume loss from Antarctic ice shelves is accelerating. *Science*, *348*(6232), 327-331.
- Paolo, F., Gardner, A. S., Greene, C. A. & Schlegel, N, 2024) MEaSURES ITS_LIVE Antarctic Quarterly 1920 m Ice Shelf Height Change and Basal Melt Rates, 1992-2017. (NSIDC-0792, Version 1). [Data Set]. Boulder, Colorado USA. NASA National Snow and Ice Data Center Distributed Active Archive Center. https://doi.org/10.5067/SE3XH9RXQWAM. Date Accessed 04-25-2025.
- Picton, H. J., Stokes, C. R., Jamieson, S. S., Floricioiu, D., & Krieger, L, 2023. Extensive and anomalous grounding line retreat at Vanderford Glacier, Vincennes Bay, Wilkes Land, East Antarctica. *The Cryosphere*, 17(8), 3593-3616.
- Pritchard, H., Ligtenberg, S. R., Fricker, H. A., Vaughan, D. G., van den Broeke, M. R., & Padman, L, 2012. Antarctic ice-sheet loss driven by basal melting of ice shelves. *Nature*, 484(7395), 502-505.
- Rignot, E., Mouginot, J., Scheuchl, B., Van Den Broeke, M., Van Wessem, M. J., & Morlighem, M, 2019. Four decades of Antarctic Ice Sheet mass balance from 1979–2017. *Proceedings of the National Academy of Sciences*, 116(4), 1095-1103.
- Scambos, T. A., Bohlander, J. A., Shuman, C. A., & Skvarca, P, 2004. Glacier acceleration and thinning after ice shelf collapse in the Larsen B embayment, Antarctica. *Geophysical Research Letters*, 31(18).
- Schoof, C, 2007. Ice sheet grounding line dynamics: Steady states, stability, and hysteresis. *Journal of Geophysical Research: Earth Surface*, 112(F3).
- Smith, B., Fricker, H. A., Gardner, A. S., Medley, B., Nilsson, J., Paolo, F. S., ... & Zwally, H. J., 2020. Pervasive ice sheet mass

loss reflects competing ocean and atmosphere processes. *Science*, *368*(6496), 1239-1242.

Weertman, J, 1974. Stability of the junction of an ice sheet and an ice shelf. *Journal of Glaciology*, *13*(67), 3-11.

Young, D. A., Wright, A. P., Roberts, J. L., Warner, R. C., Young, N. W., Greenbaum, J. S., ... & Siegert, M. J, 2011. A dynamic early East Antarctic Ice Sheet suggested by ice-covered fjord landscapes. *Nature*, 474(7349), 72-75.